Andrade, J.; González Martínez, MC.; Chiralt Boix, MA. (2020). Effect of carvacrol in the properties of films based on poly (vinyl alcohol) with different molecular characteristics. Polymer Degradation and Stability. 179:1-11. https://doi.org/10.1016/j.polymdegradstab.2020.109282

INCORPORATION OF CARVACROL INTO POLY (VINYL ALCOHOL) FILMS, AS AFFECTED BY THE POLYMER MOLECULAR CHARACTERISTICS

J. Andrade[a], C. González-Martínez[a], A. Chiralt[a]

[a] Instituto Universitario de Ingeniería de Alimentos para el Desarrollo, Universitat Politècnica de València, Camino de Vera s/n, 46022 Valencia, Spain.

Corresponding author: joancha@doctor.upv.es; cgonza@tal.upv.es; dchiralt@tal.upv.es

ABSTRACT

Polyvinyl alcohol (PVA) is a hydrophilic linear polymer obtained from the controlled hydrolysis of polyvinyl acetate (PVAc). The molecular weight (Mw) and degree of hydrolysis (DH) of PVA are considered relevant in both the functionality of the polymer and its capacity for film formation. This study analysed the influence of the Mw and DH of PVA on both the film's ability to incorporate carvacrol (CA), for the purposes of obtaining active films for food packaging application, as well as on the film microstructure and thermal behaviour and its functional properties as packaging material. CA was incorporated at 5 and 10 g/100 g polymer by emulsification in the polymer-water solutions, while the films were obtained by casting. The higher Mw polymer provided films with a better mechanical performance but less CA retention and a more heterogeneous structure. In contrast, low Mw, partially acetylated PVA gave rise to homogenous films with a higher CA content that increased the mechanical resistance and stretchability of the films. The melting temperature of this polymer with acetyl groups was lower than the degradation temperature, which makes thermoprocessing feasible.

Keywords

Molecular weight; Degree of hydrolysis; Thermal Behaviour; Cross-linking; Food packaging.

1. Introduction

The development of biodegradable packaging materials has become a matter of great importance, especially within the food sector. This industry currently reports one of the highest rates of non-biodegradable plastic consumption destined for food packaging, generating a negative impact on the environmental balance, problematic that must be counteracted through the progressive change in the packaging system [1]. Food packaging materials must meet not only determined requirements to ensure food preservation and safety: adequate barrier properties to water vapour and gases, proper mechanical performance and optical properties, along with thermal characteristics to ensure their processability, but also the requirements of environmental sustainability [2]. To this end, different biodegradable polymers (biobased or not), as well as their blends, have been evaluated and characterized. Some non-biobased, biodegradable polymers, such as poly (Ɛ-caprolactone) (PCL), poly (butylene succinate/adipate) (PBS / A), poly (butylene adipate-co-terphthalate) (PBA / T) and poly (vinyl alcohol) (PVA), have been extensively studied because of their high versatility. In these polymers, it is possible to adjust some of their molecular parameters by controlling their processing factors, thereby modifying the characteristics and functionality of the material.

Some molecular characteristics of these biodegradable polymers, such as chain length, molecular weight, number and types of functional groups or tacticity (which is related to the stereoregularity of the chain), as well as the processing conditions, are factors which determine the physical and functional properties of the resulting materials. Bhagabati et al. [2] report that the polymer crystallinity and oxygen barrier capacity and transparency of PCL films have been shown to be highly dependent on the molecular weight. The molecular and chemical structure of the PBA and the PBS were relevant factors in the thermal behaviour and in the biodegradation by enzymatic hydrolysis of these polyester films [3]. Barrera et al. [4] showed that the degree of hydrolysis of the PVA molecular chains generated significant differences in the glass

transition temperature (Tg), the melting temperature (Tm) and the thermal degradation mechanisms of the PVA films. Aruldass et al. [5] reported an increment in the crystallinity and water solubility of the PVA films when increasing the hydrolysis degree of PVA. The greater PVA crystallinity promoted, in turn, the development of smoother film surfaces.

PVA is produced by partial or complete hydrolysis of the polyvinyl acetate, eliminating the acetate groups; this means that both the molecular weight and the degree of hydrolysis of the PVA can be controlled to obtain materials with different properties and functionality [6]. The high number of hydroxyl groups in the molecular chain of PVA confers it with a highly hydrophilic nature, enhancing biocompatibility, and promotes the formation of hydrogen bonds, affecting the physical properties of the material [7]. These characteristics have encouraged the use of PVA to develop biodegradable films, using pure PVA or blended with other biopolymers, such as starch [7–12], proteins [13,14], chitosan [14–16] or cellulose and derivatives [17,18] in order to obtain biodegradable materials with adequate properties for different uses.

One relevant aspect related with food preservation is the availability of active packaging. The incorporation of active compounds, with antioxidant or antimicrobial activity, in different polymeric matrices has been studied to obtain antimicrobial or antioxidant packaging materials [19–21]. In this sense, the compatibility of the active compounds with the polymer matrix and the controlled release to the food mainly depend on the chemical nature of the compounds involved and their molecular interactions. These interactions are of great importance since they determine the applicability of the active films.

Several studies have been carried out with the aim of developing active films based on PVA using fully hydrolysed, high molecular weight polymer. Thus, kavoosi et al. [22] and Chen et al. [23] obtained active films of fully hydrolysed (1–2% acetate groups) PVA, incorporating essential oils of *Zataria multiflora* and clove, respectively.

These films exhibited effective antimicrobial and antioxidant activities in the vapour phase. Nevertheless, the low affinity between the essential oil compounds and the PVA chains negatively influenced the mechanical resistance, oxygen barrier properties and thermal stability of the films. In contrast, the incorporation of tea polyphenols in nanocomposites of PVA with Montmorillonite significantly improved the tensile strength and the water vapour and oxygen barrier capacity, due to the formation of hydrogen bonds between the polymer matrix and phenols [24]. Other studies analysed the properties of PVA-based blend films incorporating different natural active compounds, such as curcumin [25], gallic acid [26], mint and pomegranate peel extract [27]. None of these studies have evaluated the effect of the PVA molecular characteristics on the film properties and functionality.

The aim of this study was to develop and characterise active PVA films containing carvacrol (CA), by using two types of PVA with different hydrolysis degree and molecular weight. The effect of the molecular characteristics of the polymer on the CA retention in the film, the film microstructure, polymer crystallization degree, thermal behaviour and barrier and tensile properties of the films has been analysed.

2. Materials and methods

2.1. Materials

Two types of poly (vinyl) alcohol (PVA) with different molecular weight and degree of hydrolysis (A: Mw 89,000-98,000; 99-99.8% hydrolysed and B: Mw 13,000-23,000; 87-89% hydrolysed) and carvacrol were purchased from Sigma-Aldrich (Steinheim, Germany) and magnesium nitrate ($Mg(NO_3)_2$), phosphorus pentoxide (P_2O_5) salts and UV-grade methanol were supplied by Panreac Química S.A. (Barcelona, Spain).

2.2. Film preparation

The films were prepared by casting of the aqueous solution of the polymer. Polymer (A 5% wt. and B 10% wt.) solutions in distilled water were prepared using magnetic stirring (1200 rpm) at 100 °C for 3 h. CA was incorporated into the PVA solution at 5% wt. and 10% wt. (with respect to the polymer) by applying sonication (20 kHz for 5 min, with pulses of 1 s), using a ultrasonic processor (Avantor, 505-Vibra Cell, USA). All formulations were degassed by using a vacuum pump and spread evenly onto Teflon plates of 150 mm in diameter, using a constant equivalent mass of polymer per plate of 2 g. The films were dried for approximately 48 h under controlled relative humidity (RH) and temperature (T) conditions (RH: 50 ± 2% and T: 25 ± 2 ℃). Subsequently, the films were conditioned for one week at 53% RH, using $Mg(NO_3)_2$ over-saturated solution, before their characterisation. Therefore, the final CA content in the film (CA retention), microstructure and thermal analyses were carried with films conditioned at 0% RH using P_2O_5. Table 1 shows the different film formulations with the respective mass fractions of the components.

2.3. Characterisation of the active PVA films

2.3.1. CA retention and microstructure of the films

CA retained in the different formulations was determined through the extraction of CA contained in the dried films and its spectrophotometric quantification. The extraction was carried out from film samples of 4 cm^2 in area in 50 mL of a 50% (v/v) aqueous solution of UV-grade absolute methanol, and kept under stirring at 300 rpm for 48 h at 25 ℃. Absorbance (x) of the extracts was measured at 274 nm, using a spectrophotometer (Evolution 201 UV-Vis, Thermo Fisher Scientific, USA). The CA concentration (y) in the films was determined by means of a standard curve obtained with CA solutions containing between 10 and 50 µg/mL in the same solvent ($y = 63.61x, R^2 = 0.998$). The backgrounds used for the measurements were the

corresponding extracts obtained under the same conditions from the CA-free films. CA retention in the films was calculated, in percentage, as the ratio between the mass of CA extracted from the film with respect to the corresponding mass of CA initially incorporated.

The microstructure of the films was observed using a Field Emission Scanning Electron Microscope (FESEM) (ZEISS®, model ULTRA 55, Germany), at an acceleration voltage of 2 kV. The film samples were cryofractured by immersion in liquid nitrogen, platinum coated and the cross section images obtained.

The film thickness was measured with a digital electronic micrometer (Palmer, COMECTA, Barcelona, Spain) to the nearest 0.001 mm at six random positions.

2.3.2. Fourier transformed infrared spectroscopy (FT-IR)

The vibration mode of the chemical groups of the polymer was assessed in films equilibrated at 53% RH at 25 ℃ through attenuated total reflectance ATR-FTIR analysis using a Nicolet 5700 spectrometer (Thermo Fisher Scientific Inc., Waltham, MA, USA). The average spectra were collected from 64 scans with a resolution of 4 cm^{-1} in the 4000–400 cm^{-1} range. The analyses were performed in triplicate and at three different locations in each sample.

2.3.3. Thermal behaviour

The thermal behaviour of the films was characterised using thermogravimetric analysis (TGA/SDTA 851e, Mettler Toledo, Schwarzenbach, Switzerland) and differential scanning calorimetry (DSC 1 StareSystem, Mettler-Toledo, Inc., Switzerland). TGA analysis was performed by heating from 25 ℃ to 700 ℃ at 10 ℃/min under a 10 mL/min nitrogen stream. DSC curves were obtained by multiple scan. A first heating from -25 ℃ to 250 ℃ at 10 ℃/min, holding for 2 min at 250 ℃. Samples were then cooled to -25 ℃ and held for 2 min before the second heating from -25 to 250 ℃ at 10 ℃/min. Analyses were carried in triplicate for each sample.

159 *2.3.4. X-ray diffraction*

160 The X-ray diffraction spectra of the films were recorded with a D8 Advance X-
161 ray diffractometer (Bruker AXS, Karlsruhe, Germany) between 2θ: 10° and 50°, with a
162 step size of 0.05, using Kα Cu radiation (λ: 1.542 Å), 40 kV and 40.mA. The degree of
163 crystallinity (Xc) of the samples was estimated from the ratio of crystalline peak areas
164 and the integrated area of X-R diffractograms and expressed as a percentage. The
165 diffraction scattering curve was deconvoluted with Lorentz model using the OriginPro
166 8.5 software, for crystalline and amorphous peaks.

167 *2.3.5. Tensile properties*

168 Tensile properties were determined using a universal testing machine (Stable
169 Micro Systems, TA.XT plus, Haslemere, England), following the standard method
170 ASTM D882-02 [28]**.** For each formulation, eight test specimens (25 mm x 100 mm)
171 were cut and conditioned for one week (RH: 53% and T: 25 ℃) and subjected to the
172 extension test. The initial separation of the clamps was 50 mm and elongation speed
173 50 $mm.min^{-1}$. From the stress (σ)-Henky deformation (ε_H) curves, the elastic modulus
174 (EM) and tensile strength (TS) and elongation at break point (E) were obtained.
175 Measurements were carried out 8 times for each sample.

176 *2.3.6. Barrier properties*

177 Water vapour permeability (WVP) was analysed following a modification of the
178 E96/E95M-05 gravimetric method [29]. The film samples of each formulation were
179 placed on Payne permeability cups (3.5 cm in diameter, Elcometer SPRL, Hermelle/s
180 Argentau, Belgium) at 25 ℃ and 53-100% RH gradient, which was created with an
181 oversaturated $Mg(NO_3)_2$ solution (inside the desiccator where cups were placed) and
182 distilled water (5 mL inside the cup). In order to reduce the resistance to transport of
183 water vapour, a fan was positioned above each cup. The cups were weighed
184 periodically every 1.5 h for 24 h using an analytical balance (±0,00001 g). To calculate

185 WVTR, the slopes in the steady state period of the weight loss *vs.* time curves were
186 determined by linear regression. WVP was calculated according to Cano et al. [30]. For
187 each type of film, WVP measurements were carried out in triplicate.

188 The oxygen permeability (OP) was determined following a modification of the
189 standard method F1927-07 [31]. For this analysis, the Ox-Tran system (Mocon,
190 Minneapolis, US) at 23 ℃ and 53% RH was used. Sample films (50 cm^2) were exposed
191 to pure nitrogen flow on one side and pure oxygen flow on the other side. OP was
192 calculated by dividing the oxygen transmission rate by the partial pressure of oxygen
193 and multiplying it by the average film thickness. Each film formulation was analysed in
194 triplicate.

195 *2.3.7. Optical properties*

196 The optical properties (transparency and colour coordinates) were determined
197 by measuring the reflectance spectra of the samples from 400 to 700 nm, on white (R)
198 and black (R_0) backgrounds, as well as the reflectance of the white backing (R_g), using
199 a spectrocolorimeter (CM-3600d Minolta CO., Tokyo, Japan). Three measurements
200 were taken from each film and three films were considered per formulation. The
201 transparency was measured through the internal transmittance (Ti), applying the
202 Kubelka-Munk theory for multiple scattering (Eq. 1). The CIE L*a*b* colour coordinates
203 were obtained from the reflectance of an infinitely thick film (R_∞) (Eq. 2) spectra, by
204 using D65 illuminant and observer 10°, observer according to Hutchings (1999).
205 Psychometric coordinates, Chroma (C_{ab}*) and hue (h_{ab}*) were also determined using
206 Eqs. (5) and (6).
207

$$T_i = \sqrt{(a + R_0)^2 - b^2} \quad (1)$$

$$R_\infty = a - b \quad (2)$$

$$a = \frac{1}{2}\left[R + \frac{R_0 - R + R_g}{R_0 \times R_g}\right] \quad (3)$$

$$b = (a^2 - 1)^{1/2} \quad (4)$$

$$C^*_{ab} = \sqrt{(a^{*2} + b^{*2})} \quad (5)$$

$$h^*_{ab} = arctg\,\frac{b^*}{a^*} \quad (6)$$

208

209 *2.4. Statistical analysis*

210 The statistical analysis of the data was carried out using Statgraphics Centurion
211 XVI.II. The results were submitted to an analysis of variance (ANOVA). Fisher`s least
212 significant difference (LSD) was used at the 95% confidence level.

213

214 **3. Results and discussion**

215 *3.1. Film microstructure and carvacrol retention.*

216 The percentages of CA retention and final CA contents in the two types of PVA
217 films are shown in Table 1. The type of PVA significantly affected the final content of
218 CA in the films, the compound retention being higher in the matrix with lower degree of
219 hydrolysis (B). This may be attributed to the greater compound affinity with the polymer
220 chains due to the presence of residual acetyl groups, which confer a more hydrophobic
221 nature on the polymer. Films obtained by the casting of aqueous solutions of
222 hydrophilic polymers, containing essential oils, lose a great part of the emulsified oil
223 during the drying step because of the emulsion destabilization (droplet flocculation,

coalescence and creaming) and steam drag of the surface oil in line with water evaporation [32]. Factors improving the emulsion stability, such as the presence of amphiphilic compounds or high viscosity, mitigate these losses [32]. Likewise, a greater affinity between the essential oil compounds and the polymer chain can favour the bonding of active compounds in the polymer matrix, increasing their retention in the film.

Table 1. Nominal fraction (x) of the different components in the different film formulations, CA content in the final films (extracted) and retention percentage. Mean values and standard deviation.

Sample	x_{PVA}	x_{CA}	CA extracted from the films		CA-Retention (%)
			(mg CA/ g dry film)	(mg CA/ g polymer)	
A	1	-	-	-	-
A-CA5	0.95	0.05	23 ± 1^{a}	24 ± 1^{a}	48 ± 2^{a}
A-CA10	0.91	0.09	46 ± 2^{c}	51 ± 2^{c}	51 ± 2^{a}
B	1	-	-	-	-
B-CA5	0.95	0.05	28 ± 2^{b}	29 ± 1^{b}	58 ± 3^{b}
B-CA10	0.91	0.09	57 ± 2^{d}	63 ± 2^{d}	**63. 2^{c}**

Different superscript letters within the same column indicate significant differences among films (P<0.05).

***(2-columns)**

The microstructural analysis permits the identification of the arrangement of the different components in the film, which can be correlated with the film's functional properties, such as barrier, mechanical or optical. During the film drying step, the solvent evaporation leads to an increase in both the viscosity of the continuous phase and in the concentration of the dispersed phase that affect the kinetics of the destabilization process of emulsified film forming systems. This leads to changes in the

particle size distribution of the dispersed lipid fraction, affecting the internal structure of the film and the final properties of the film matrix [19,33]. The cross section of the obtained films (Figure 1) showed marked differences in the internal structure for A and B polymers, which may be related with their different chemical affinity with CA and the viscosity of the film-forming systems.

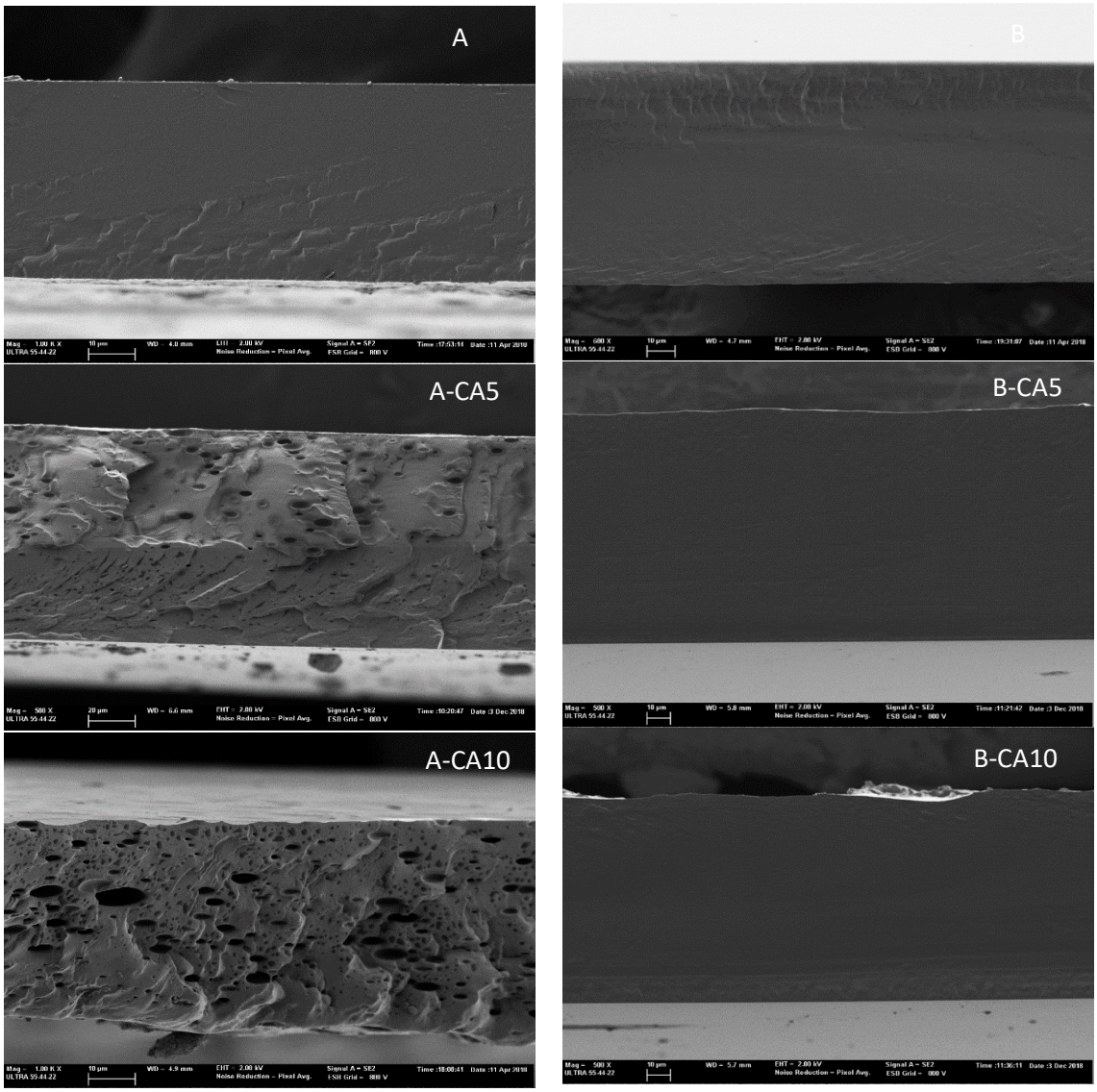

Figure 1. FESEM micrographs of the cross-section of the PVA films (A and B) without and with carvacrol (5 or 10 g/100 g PVA).

***(2-columns)**

In films from fully hydrolysed PVA (A), CA was distributed stochastically in droplets of highly variable sizes, whereas no lipid droplets were observed in partially acetylated PVA (B) despite the higher CA content determined in the latter case. The high degree of hydrolysis and the longer size of the chains favour the chain intermolecular forces in polymer A, leading to greater cohesion forces in the matrix, whereas the chemical affinity with CA is lower than in polymer B. This low chemical affinity provokes the CA phase separation (visible droplets), as observed in Figure 1, and limits its retention in the matrix. This effect was also reported by other authors [23] in PVA films (with the same M_W and degree of hydrolysis) for clove oil at concentrations higher than 3%. The lack of visible CA droplets in films from polymer B, with higher final CA content, suggests that the remaining CA is bonded to the polymer chains, generating a homogeneous structure able to link a determined amount of the compound without phase separation in the matrix. The smaller molecular weight of polymer B imparts lower viscosity to the film-forming systems which should limit the system's ability to stabilise the emulsified CA against creaming and its subsequent losses by steam drag effect during the film drying step. However, the acetylated groups in the chains could favour the bonding of CA molecules by chemical interactions in a non-emulsified form. As reported by Wiśniewska et al. [34], acetyl groups in the chains ionize (Figure 2), generating negative charges (lone electron pairs) that can act as electron donors (Lewis base). On the other hand, the hydroxyl group of CA, acting as Lewis acid, could form Lewis adducts with the lone electron pairs of negatively charged PVA chains. This reaction could contribute to the higher CA retention in matrix B, without phase separation, as observed in Figure 1. In fact, taking into account the molar ratio between CA and acetylated groups of PVA (B), deduced from the degree of hydrolysis and the mass ratio of CA and polymer, an excess of acetylated groups could be deduced for both 5 and 10 g CA/ 100 g polymer (7 and 3.6 moles of acetylated groups / CA mole, respectively). Therefore, the evident differences in the film

281 microstructure and CA retention between the two types of PVA must be attributed to
282 the different degree of hydrolysis and molecular weight of the polymer chains.

283

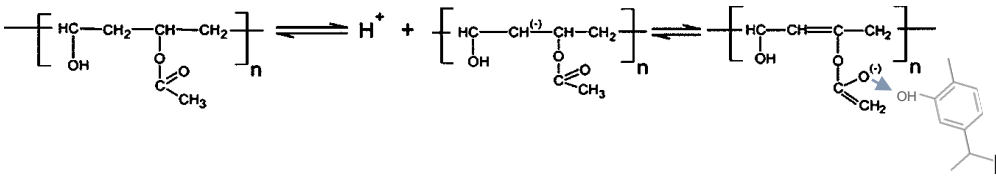

284 **Fig**

285 **ure 2.** Ionization mechanism of acetylated PVA chains [34] and proposed Lewis adduct
286 formation with carvacrol.

287 ***(2-columns)**

288

289 FTIR spectra (Figure 3) of the films have been obtained to analyse possible
290 changes in the molecular vibration modes associated with the interactions with CA. All
291 spectra of polymer A films show a similar pattern. The spectra show the typical broad
292 peak at 3260 cm^{-1} associated with the intermolecular hydrogen bonding and the
293 hydroxyl (O-H) stretching vibration. The C-H asymmetrical and symmetrical stretching
294 vibration occurs at 2930 cm^{-1} and 2910 cm^{-1}, respectively. Other peaks appear at
295 1416 cm^{-1}, 1326 cm^{-1}, 1085 cm^{-1} and 832 cm^{-1}, which are related to CH_2 bending,
296 motion of the carbon skeleton (C-H), C-O stretching and C-C stretching [7,24,35]. FTIR
297 spectra of films from partially acetylated polymer B presented the same peaks, slightly
298 displaced, with three additional peaks associated with the stretching vibrations bands
299 of the carbonyl (C=O) and acetyl groups that were observed at 1732 cm^{-1}, 1372 cm^{-1}
300 and 1240 cm^{-1}.

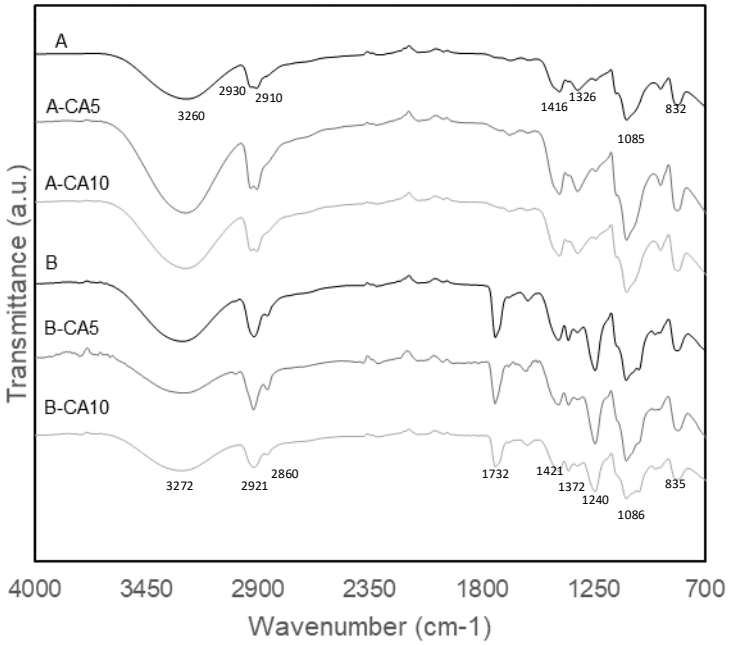

Figure 3. FTIR spectra of the PVA films (A and B) without and with carvacrol (5 or 10 g/100 g PVA).

***(Single column)**

In neither case did the presence of CA cause changes in the vibration band of PVA. Not even the described interaction between CA and acetyl groups in PVA B chains caused changes in the vibration mode of carbonyls. This can be attributed to the very low molar ratio of CA in the films, which prevents the quantitative observation of its characteristic vibration bands, and the lack of covalent interactions between CA and PVA groups affecting the vibration mode of the chain bonds. The characteristic FTIR peaks of carvacrol have been observed by other authors [36–39] at 3500-3300 cm^{-1} (O-H stretch), 2868-2958 cm^{-1} (C-H stretch), 1620-1485 cm^{-1} (C-C stretch), 1240 cm^{-1} (C-O stretching vibration in aromatic ring) and 800 cm^{-1} (aromatic C-H bending).

3.2. Thermal behaviour and crystallinity of the films

The DSC analysis was carried out in two heating steps, whose thermograms are shown in Figure 4. The presence of first and second order transitions in all samples corroborates the semi-crystalline character of the PVA in the film samples. The first heating scan reflects the state of the polymer after the casting process, while the second heating scan shows the thermal behaviour of the material once its previous thermal history has been erased by the polymer melting in the first heating step. Table 2 shows the temperature and enthalpy values for the different thermal events shown in Figure 4.

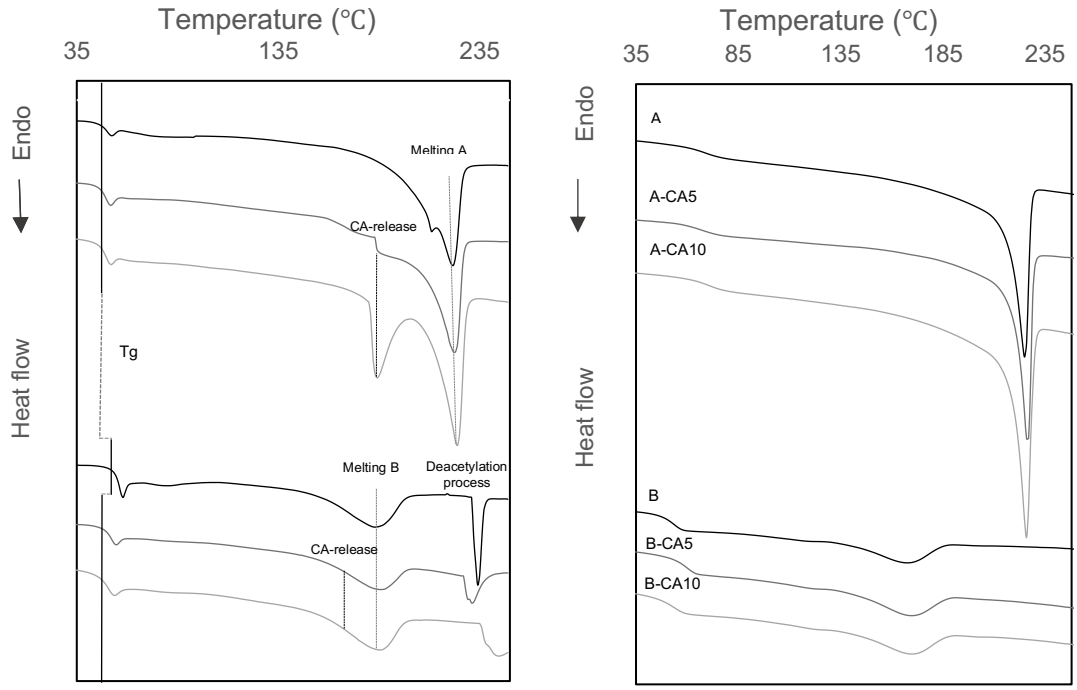

Figure 4. DSC curves of the PVA films (A and B) without and with carvacrol (5 or 10 g/100 g PVA). On the left, the first heating scan and on the right the second heating scan.

***(2-columns)**

Glass transition temperature (Tg) between 48-53 ℃ appeared in both polymers (A and B), where a relaxation enthalpy can be observed in the first heating step

associated with the polymer ageing during storage [40]. In the first heating step, the Tg values of polymer A were lower than those of polymer B despite the latter's lower molecular weight. This could be attributed to different factors, such as the greater restrictions in the molecular mobility imposed by the acetyl groups in the amorphous phase generated during casting or to the differences in the bonded water that can plasticise the matrix to a different extent. Due to the slow process of film formation by casting (in line with water evaporation), macromolecules of different molecular weight in each polymer solution could be preferably located in the amorphous phase due to the different crystallization restrictions associated with the steric hindrance in the molecular arrangement. The lowest molecular weight chains seem to preferably constitute the amorphous phase of matrix A, whereas the opposite behaviour seems to occur for the partially acetylated polymer B. The high content of bonded water in polymer A, commented on below, can also have a plasticising effect on matrix A, thus decreasing the Tg value. In this sense, it is remarkable that Tg values of polymer A were higher (73 ℃) once the bonded water was eliminated during the first heating and the polymer melted and recrystallized in the melt (second heating step). This notable variance in Tg values suggests a different average molecular weight of the macromolecules constituting the amorphous phase both in cast films and after melting and heating till 250 ℃. For polymer B, the Tg values were only slightly higher in the second heating step, which could be mainly attributed to the loss of bonded water during the first heating, with the formation of an amorphous phase of similar composition to that formed in cast films.

No effect of the CA incorporation on the Tg values of polymer A was observed, although CA plasticised matrix B, decreasing the Tg values of the polymer in cast films (first heating), in agreement with the previously described interactions between CA and acetylated PVA. These interactions can enhance the free volume of the chains, promoting molecular mobility. In the second heating, no significant differences in Tg

values were observed for the different samples obtained with polymer B, which confirms the CA delivery during the first heating.

Both polymers exhibited several endotherms events between 180 ℃ and 240 ℃ that can be attributed to the polymer melting, CA evaporation or endothermic degradation events as the temperature increases. To better understand the origin of these events, the TGA and DGTA curves (Figure 5), showing the different weight loss steps, were taken into account. This is because both the CA losses detected in TGA, as well as some incipient thermodegradation steps of the polymer, could imply endothermic peaks. TGA and DTGA curves exhibit notable differences between the thermal behaviour of samples from polymers A and B. In both cases, DTGA curves showed a first weight loss step corresponding to the loss of bonded water in the polymer matrix (conditioned at 0% RH): 3% of bonded water was lost by the non-acetylated polymer A, while only 1.5% of bonded water was determined for matrices B, in agreement with their more hydrophobic nature provided by acetyl groups. The second weight loss step of TGA curves, which only appears in samples containing CA, must be attributed to the CA thermo-release at about 196 ℃ and 150 ℃ for polymers A and B, respectively. The amount of CA released in this step ranged between 40-60% of the final CA content determined in the films and it is remarkable that no quantitative mass of CA was released at 196 ℃ in sample A with 5% nominal CA content. However, a very small endothermic event was detected in the first heating step of the DSC before the melting endotherm.

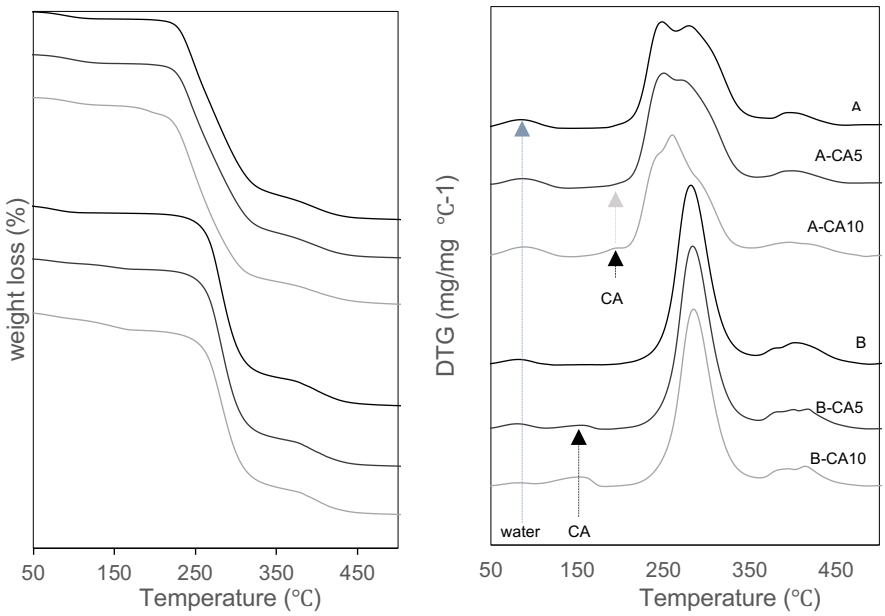

381

382 **Figure 5.** TGA (left) and DTGA (right) curves of the PVA films (A and B) without and with
383 carvacrol (5 or 10 g/100 g PVA).

384 ***(2-columns)**

385

386 The earlier partial release of CA in polymer B at about 150 ℃ could be due to
387 the lower melting temperature of this polymer (Tm: 180 ℃, first heating step in Table
388 2) than that of polymer A (Tm: 225 ℃). The carvacrol release that occurred was
389 associated with the polymer melting and this event could affect the melting enthalpy of
390 polymer B in the first DSC heating step. Likewise, the first endotherm, at about 190 ℃
391 in samples A containing CA, must be attributed to the CA evaporation, as deduced
392 from the TGA detection of the CA thermo-release at this temperature.

393 A second endotherm, at between 230-245 ℃, appeared in the first heating step
394 for samples B that could be attributed to endothermic events associated with polymer
395 thermodegradation, such as the deacetylation process, as reported by other authors
396 [41,42]. Deacetylation is autocatalytic and corresponds to the first degradation
397 mechanism of acetylated PVA and, in inert conditions (N_2 flow), the deacetylation step
398 as well as the chain scission reaction show endothermic effects. In DGTA curves, the

399 polymer B degradation process starts at about 220 ℃ under N_2 flow. Then,
400 endothermic degradation events are reflected in the first heating step of DSC curves
401 (Figure 4).

402

403 **Table 2.** Glass transition and melting temperature and enthalpy of the PVA films (A and B)
404 without and with carvacrol (5 or 10 g/100 g PVA).

	First heating scan			Second heating scan		
	Tg (℃)	Tm(℃)	ΔHm (J.g-1)	Tg (℃)	Tm (℃)	ΔHm (J.g-1)
A	48.0 ± 0.2a	225 ± 5b	78.6 ± 0.4c	73 ± 3b	225 ± 1b	74 ± 3b
A-CA5	48.1 ± 0.2a	224 ± 2a	72 ± 2c	74 ± 3b	226 ± 1b	69 ± 3b
A-CA10	48.1 ± 0.1a	223 ± 1a	63 ± 3b	71 ± 3b	225 ± 1b	71 ± 7b
B	53.8 ± 0.4c	183 ± 1a	40 ± 4a	56 ± 3a	168 ± 1a	25 ± 2a
B-CA5	49.9 ± 0.8b	184 ± 2a	37 ± 6a	58 ± 6a	168 ± 1a	22 ± 1a
B-CA10	49 ± 2ab	184 ± 1a	39 ± 2a	53 ± 2a	169 ± 1a	23 ± 2a

405 Different superscript letters within the same column indicate significant differences among films ($p<0.05$).

406 ***(2-columns)**

407

408 The degradation of the polymeric material occurred in two stages; the first
409 started at about 200 ℃ (A) or 220 ℃ (B) and represented around 70% of the weight
410 loss of the samples and the second stage started at 360 ℃ with about 12% of weight
411 loss. The temperature peak of the first main step was 248 ℃ for polymer A and 281 ℃
412 for polymer B. For the acetylated chains, such as polymer B, the detachment of acetyl
413 groups from the chains, forming water, acetaldehyde and acetic acid, has been
414 described as the first degradation mechanism [4]. For polymer A, the degradation
415 peak in DGTA curves showed an overlapping of different weight loss events,
416 suggesting the action of different simultaneous degradation events. This could be
417 related with the fact that both the melting of the crystalline fraction (Tm: 225 ℃) and
418 degradation occur in the same temperature range and melt and crystalline phases

should degrade differently. In contrast, the degradation of polymer B occurred once melted above 180 ℃ (Table 2) in a more continuous degradation process. The second stage of polymer degradation above 360 ℃ was related to the degradation of low molecular weight products from the decomposition of the main chain, or of heavier structures formed in the previous degradation stage [4].

Thus, molecular properties of PVA affected the thermal behaviour of the material. The degree of hydrolysis of the polymer was highlighted, since the acetate groups in the B-chains appear to have a thermo-protective effect, as described by Cristancho et al. [43], who report that the presence of the carbonyl group (C=O) in the PVA-chains increases the absolute value of the energy required for the material degradation. In this sense, Barrera et al. [4] applied both the Friedman and the Freeman-Carroll methods to determine the activation energy (E_a) of PVA degradation, and found that E_a was inversely proportional to the degree of hydrolysis of the polymer. This is of particular importance for the feasibility of the thermal processing of polymers. Thermoprocessing requires the melting temperature to be rather lower than the degradation temperature. This occurs in acetylated low molecular weight PVA (B) but not in fully hydrolysed high molecular weight PVA, which could not be submitted to the thermoplastic industrial processes because it has no adequate thermal processing window. In the second heating step of the DSC analysis, a part of PVA A would be degraded, since the temperature of the first heating reached 250 ℃. So, both the obtained values of Tg and Tm would be affected by this partial degradation. In fact, the much higher values of Tg obtained in the second heating could be due to the higher mean molecular weight of the remaining molecules. The melting temperature coincides with the value of the first heating step, which suggests that no significant changes in the crystalline fraction occurred as a result of the partial degradation at 250 ℃.

Other authors [6,7] only reported Tg and Tm values from the second heating step of the DSC analysis under similar conditions, which agree with those found in this study. Nevertheless, during the first heating, the state of the polymer was modified by both melting above Tm and partial thermogradation. So, the second heating DSC analysis did not reflect the real polymer state in cast films. The melting enthalpy values and melting temperature of polymer B in particular were higher for the cast samples (first heating) than for the melt samples (second heating), which could point to the formation of bigger, more stable crystals in cast films due to the greater mobility of molecules in the water solution than in the melt.

The crystallinity of PVA in the cast films was analysed by DRX analysis, since the different overlapped endothermic events occurring during DSC analyses did not permit its evaluation from the melting enthalpy data. The DRX patterns of pure PVA-films and PVA-films with different CA ratios are shown in Figure 6. PVA films showed a crystalline peak at around $2\theta = 19.7°$ with a shoulder at 22.6° and a small broad peak at 41.5°. The B-films showed a slight decrease in the crystalline peak's intensity and an increase in the width of the main crystalline peak with respect to the A-films, which suggests a lower percentage of crystallinity and smaller crystals in polymer B [44]. The crystallinity quantified through the peak area is indicated in Figure 6 for each sample and was higher for polymer A than for polymer B, both slightly increasing when CA was present. The greater crystallinity of polymer A can be explained by the more homogenous chain structure (without acetyl groups) that enhances both the capacity to form inter-chain hydrogen bonds and the crystalline arrangement. Polymer B, with partially acetylated chains, has steric hindrance that limits a more ordered, crystalline molecular organization.

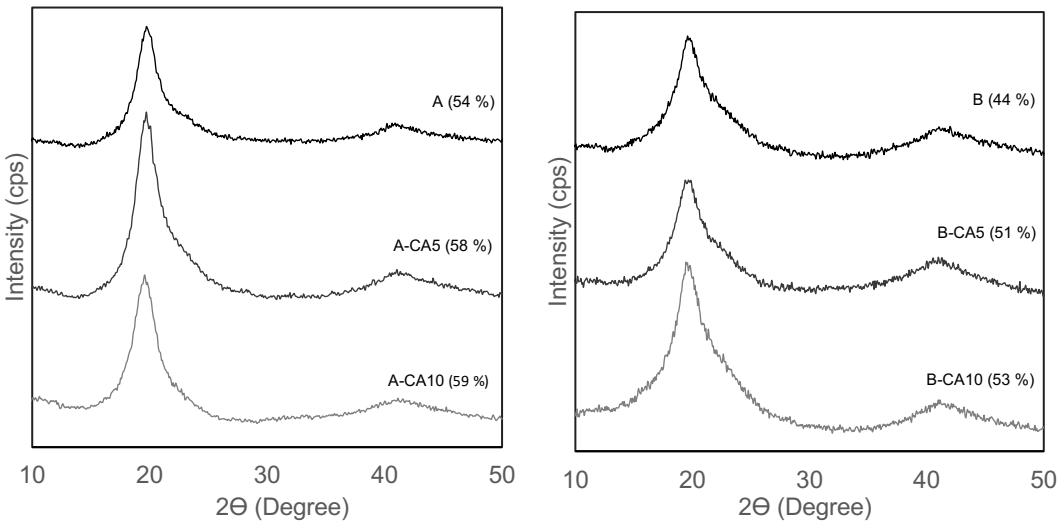

Figure 6. X-Ray diffraction spectra of the PVA films (A and B) without and with carvacrol (5 or 10 g/100 g PVA). Percentages of crystallinity are shown for each sample.

***(2-columns)**

3.3. Tensile, barrier and optical properties of the films.

Table 3 shows the values of tensile parameters (elastic modulus: EM, tensile strength: TS and elongation: E, at break) of the different films. Films obtained with polymer A exhibited better mechanical performance than those with B, which can be attributed to the formation of more inter-chain hydrogen bonds due to the longer molecular chains with a greater proportion of hydroxyl groups. In contrast, the acetyl groups in polymer B interrupted the hydrogen bond formation in the shorter chains. This limits the cohesion forces in the matrix and reduces the mechanical performance of the material. Restrepo et al. [45] also found that the increase in molecular weight and the degree of hydrolysis improved the mechanical properties of the PVA materials.

Table 3. Thickness, tensile parameters (Tensile strength (TS), elongation (E), at break and elastic modulus (EM)) and barrier properties (water vapour permeability: WVP and oxygen

488 permeability: OP) of the PVA films (A and B) without and with carvacrol (5 or 10 g/100 g PVA).
489 Mean values and standard deviation.

Sample	Thickness (μm)	TS (MPa)	E (%)	EM (MPa)	WVP x 10^3 (g/m. h. kpa)	OP x 10^8 (cm^3/m. h. kpa)
A	101 ± 2^{bc}	153 ± 8^{d}	135 ± 6^{c}	80 ± 4^{b}	2.47 ± 0.06^{a}	0.38 ± 0.01^{a}
A-CA5	106 ± 2^{c}	138 ± 13^{c}	133 ± 5^{c}	79 ± 5^{b}	2.60 ± 0.30^{a}	1.07 ± 0.10^{c}
A-CA10	108 ± 2^{a}	134 ± 5^{c}	132 ± 5^{c}	82 ± 6^{b}	3.10 ± 0.60$_{b}$	1.55 ± 0.04$_{e}$
B	95 ± 2^{b}	44 ± 6^{a}	97 ± 6^{a}	54 ± 5^{a}	2.90 ± 0.02$_{ab}$	0.53 ± 0.05^{b}
B-CA5	101 ± 2^{bc}	68 ± 4^{b}	121 ± 7^{b}	53 ± 4^{a}	3.12 ± 0.03$_{b}$	1.40 ± 0.06^{d}
B-CA10	99 ± 2^{b}	66 ± 3^{b}	118 ± 4^{b}	50 ± 3^{a}	2.45 ± 0.05^{a}	6.11 ± 0.06$_{f}$

490 Different superscript letters within the same column indicate significant differences among samples ($p<0.05$).

491 ***(2-columns)**

492

493 The incorporation of CA did not affect the elastic modulus (EM) or extensibility
494 (E) of films from polymer A, but reduced their resistance to break (TS), as previously
495 reported by Chen et al. [23] for PVA (99% hydrolysed) matrices with incorporated clove
496 oil (CO). This must be attributed to the presence of a lipid dispersed phase (Figure 1)
497 that interrupted the polymer network and weakened its mechanical resistance. In
498 contrast, the incorporation of CA into the B matrices increased the film's resistance
499 (TS) and elongation (E), without modifying EM. The CA bonded to polymer B enhanced
500 the chain slippage during stretching, making the films more extensible without break.
501 Then, the greater chemical affinity of CA with polymer B gave rise to monophasic films,
502 where CA acted by enhancing their mechanical performance. Tongnuanchan et al.
503 [46] reported that some compounds in essential oils might be able to improve the
504 polymer tensile properties due to the rearrangement of the polymer network in line with
505 the developed molecular interactions. In this sense, some studies reported an increase

506 in the TS of soy protein isolate films [47] and chitosan films [48] when cinnamon
507 essential oil was incorporated into the matrices.

508 Water vapour permeability (WVP) and oxygen permeability (OP) are relevant
509 properties for the applicability of the films as food packaging materials. These should
510 be as low as possible to prevent the accelerated degradation of products due to the
511 permeation of water vapour or other gases, such as oxygen [49]. Films from polymer A
512 exhibited a better barrier capacity against both water vapour and oxygen than film B,
513 due to the formation of a more cohesive matrix, as commented on above. Likewise, as
514 occurred in the mechanical behaviour, a different effect was provoked in each matrix by
515 the incorporation of CA. This implied a slight increase in the WVP for the A matrices,
516 whereas no significant changes were observed for matrix B. The different structural
517 arrangement of CA, previously commented on, affected the response of the matrices to
518 the transfer of water molecules.

519 As concerns the oxygen barrier capacity, an increase in OP was observed in
520 both A and B films when CA was present in the film. In both cases, the higher the CA
521 content, the higher the OP. Given that PVA exhibited a good oxygen barrier capacity, in
522 line with its hydrophilic nature, the incorporation of non-polar compounds, with an
523 increased oxygen solubility, represented a negative effect in the material barrier
524 capacity. This effect was more marked in the B films with the highest content of CA
525 (10%), probably due to the observed plasticizing action that promoted molecular
526 mobility and mass transfer processes.

527 The colour parameters of Lightness (L *), Chrome (C_{ab} *) and hue (h_{ab} *) of the
528 different samples and the internal transmittance values at 460 nm (T_i), used as a
529 transparency indicator, are shown in Table 4. Films from polymer B were lighter with
530 lower hue values than those of polymer A; this is probably due to the different
531 refractive indexes of the matrices, of differing compactness, which affect the light
532 interactions. The presence of CA in the A films slightly reduced the lightness, chrome

values and transparency (Ti) in line with the CA concentration. However, this did not significantly affect these values in the B films. This agrees with the formation of a dispersed CA phase in the A matrices (Figure 1) which provoked light scattering, reducing the film transparency and affecting the colour parameters. In the homogenous B matrices containing carvacrol, no significant effect of the compound was observed on the film optical properties.

Table 4. Lightness (L *), chrome (Cab *), hue (hab *) and internal transmittance values at 460 nm (Ti) of the of the PVA films (A and B) without and with carvacrol (5 or 10 g/100 g PVA). Mean values and standard deviation.

Sample	L*	C_{ab}*	h_{ab}*	T_i (460 nm)
A	88 ± 2^{b}	3 ± 1^{b}	114 ± 11^{c}	0.86 ± 0.01^{bc}
A-CA5	87 ± 2^{b}	3.5 ± 0.7^{b}	112 ± 3^{bc}	0.85 ± 0.01^{b}
A-CA10	82 ± 2^{a}	2.7 ± 0.4^{a}	120 ± 5^{d}	0.83 ± 0.01^{a}
B	92 ± 1^{c}	3.4 ± 0.5^{b}	104 ± 2^{a}	0.86 ± 0.01^{bc}
B-CA5	92 ± 2^{c}	2.7 ± 0.5^{a}	108 ± 5^{ab}	0.85 ± 0.01^{c}
B-CA10	92 ± 1^{c}	2.9 ± 0.4^{ab}	106 ± 2^{a}	0.85 ± 0.01^{bc}

Different superscript letters within the same column indicate significant differences among films ($p<0.05$).

***(2-columns)**

64. CONCLUSION

The molecular weight and degree of hydrolysis of the PVA significantly affected both the microstructure of the films containing carvacrol and the thermal behaviour of the polymer matrices. Semicrystalline structures were obtained in cast films from both polymers, the crystallinity being slightly higher in de-acetylated high Mw polymer. Low Mw, partially acetylated PVA melts at a lower temperature than high Mw polymer while

its thermodegradation occurs at a higher temperature due to the protective effect of acetyl groups. This makes it possible for the polymer thermoprocessing to obtain films by means of the usual thermoplastic industrial process. Likewise, the presence of acetyl groups in the chain promoted chemical affinity with active compounds, such as carvacrol, permitting a greater retention in the matrix and, thus a more effective way of obtaining active films for food packaging. This better chemical affinity between the active compound and polymer chains gave rise to homogenous films (without phase separation) that positively affected the tensile and optical properties of the films. No relevant differences between the water vapour and oxygen barrier capacity of either kind of PVA films were observed and, although the mechanical performance of the high Mw PVA films was better than that of the low Mw, partially acetylated PVA films, the incorporation of carvacrol enhanced the resistance to break and stretchability in the latter, but negatively affected the cohesion forces (elastic modulus) of the matrix in the former. Therefore, low Mw, partially acetylated PVA (B) is of great potential for the production of active films with CA, by casting or thermoprocessing, with a broader range of possible uses than high Mw, de-acetylated PVA.

Acknowledgement

The authors would like to thank the financial support from the Ministerio de Economía y Competitividad (MINECO) of Spain, through the project AGL2016-76699-R. Author Johana Andrade thanks the Departamento de Nariño-Colombia y la Fundación CEIBA for the doctoral grant. The authors also thank the services rendered by the Electron Microscopy Service of the UPV.

References

[1] European Bioplastics, Bioplastic market data 2016, Available at: http://www.european-bioplastics.org/news/publications/, (2017) 4. http://docs.european-bioplastics.org/publications/EUBP_Bioplastics_market_data_report_2016.pdf.

[2] P. Bhagabati, D. Hazarika, V. Katiyar, Tailor-made ultra-crystalline, high molecular weight poly(ε-caprolactone) films with improved oxygen gas barrier and optical properties: a facile and scalable approach, Int. J. Biol. Macromol. 124 (2019) 1040–1052. doi:10.1016/j.ijbiomac.2018.11.199.

[3] Z. Bai, K. Shi, T. Su, Z. Wang, Correlation between the chemical structure and enzymatic hydrolysis of Poly(butylene succinate), Poly(butylene adipate), and Poly(butylene suberate), Polym. Degrad. Stab. 158 (2018) 111–118. doi:10.1016/j.polymdegradstab.2018.10.024.

[4] J.E. Perilla, Estudio de la degradación térmica de poli (alcohol vinílico) mediante termogravimetría y termogravimetría diferencial thermogravimetry and differential thermogravimetry, 27 (2007) 100–105.

[5] S. Aruldass, V. Mathivanan, A.R. Mohamed, C.T. Tye, Factors affecting hydrolysis of polyvinyl acetate to polyvinyl alcohol, J. Environ. Chem. Eng. 7 (2019) 103238. doi:10.1016/j.jece.2019.103238.

[6] J. David, R. Salazar, Study of Structural, Thermic, μ-Raman and Optic Transformation of PVA/TiO2 Polymeric Membranes, Sci. Tech. 23 (2019) 543–552. doi:10.22517/23447214.15771.

[7] A. Cano, E. Fortunati, M. Cháfer, J.M. Kenny, A. Chiralt, C. González-Martínez, Properties and ageing behaviour of pea starch films as affected by blend with poly(vinyl alcohol), Food Hydrocoll. 48 (2015) 84–93.

603 doi:10.1016/j.foodhyd.2015.01.008.

604 [8] F. Kahvand, M. Fasihi, Plasticizing and anti-plasticizing effects of polyvinyl
605 alcohol in blend with thermoplastic starch, Int. J. Biol. Macromol. 140 (2019)
606 775–781. doi:10.1016/J.IJBIOMAC.2019.08.185.

607 [9] A.A. Aydin, V. Ilberg, Effect of different polyol-based plasticizers on thermal
608 properties of polyvinyl alcohol:starch blends, Carbohydr. Polym. 136 (2016)
609 441–448. doi:10.1016/j.carbpol.2015.08.093.

610 [10] D. Domene-López, M.M. Guillén, I. Martin-Gullon, J.C. García-Quesada, M.G.
611 Montalbán, Study of the behavior of biodegradable starch/polyvinyl alcohol/rosin
612 blends, Carbohydr. Polym. 202 (2018) 299–305.
613 doi:10.1016/j.carbpol.2018.08.137.

614 [11] F.F. Hilmi, M.. Wahit, N.. Shukri, Z. Ghazali, A.Z. Zanuri, Physico-chemical
615 properties of biodegradable films of polyvinyl alcohol/sago starch for food
616 packaging, Mater. Today Proc. 16 (2019) 1819–1824.
617 doi:10.1016/j.matpr.2019.06.056.

618 [12] H. Tian, J. Yan, A.V. Rajulu, A. Xiang, X. Luo, Fabrication and properties of
619 polyvinyl alcohol/starch blend films: Effect of composition and humidity, Int. J.
620 Biol. Macromol. 96 (2017) 518–523. doi:10.1016/j.ijbiomac.2016.12.067.

621 [13] B.R.B. Lara, A.C.M.A. Araújo, M.V. Dias, M. Guimarães, T.A. Santos, L.F.
622 Ferreira, S.V. Borges, Morphological, mechanical and physical properties of new
623 whey protein isolate/ polyvinyl alcohol blends for food flexible packaging, Food
624 Packag. Shelf Life. 19 (2019) 16–23. doi:10.1016/J.FPSL.2018.11.010.

625 [14] J. Ghaderi, S.F. Hosseini, N. Keyvani, M.C. Gómez-Guillén, Polymer blending
626 effects on the physicochemical and structural features of the chitosan/poly(vinyl
627 alcohol)/fish gelatin ternary biodegradable films, Food Hydrocoll. 95 (2019) 122–

132. doi:10.1016/J.FOODHYD.2019.04.021.

[15] Y.-F. Tang, Y.-M. Du, X.-W. Hu, X.-W. Shi, J.F. Kennedy, Rheological characterisation of a novel thermosensitive chitosan/poly(vinyl alcohol) blend hydrogel, Carbohydr. Polym. 67 (2007) 491–499. doi:10.1016/J.CARBPOL.2006.06.015.

[16] T. Thanyacharoen, P. Chuysinuan, S. Techasakul, P. Nooeaid, S. Ummartyotin, Development of a gallic acid-loaded chitosan and polyvinyl alcohol hydrogel composite: Release characteristics and antioxidant activity, Int. J. Biol. Macromol. 107 (2018) 363–370. doi:10.1016/j.ijbiomac.2017.09.002.

[17] V.S. Ghorpade, R.J. Dias, K.K. Mali, S.I. Mulla, Citric acid crosslinked carboxymethylcellulose-polyvinyl alcohol hydrogel films for extended release of water soluble basic drugs, J. Drug Deliv. Sci. Technol. 52 (2019) 421–430. doi:10.1016/J.JDDST.2019.05.013.

[18] P. Cazón, G. Velázquez, M. Vázquez, Characterization of bacterial cellulose films combined with chitosan and polyvinyl alcohol: Evaluation of mechanical and barrier properties, Carbohydr. Polym. 216 (2019) 72–85. doi:10.1016/j.carbpol.2019.03.093.

[19] L. Atarés, A. Chiralt, Essential oils as additives in biodegradable films and coatings for active food packaging, Trends Food Sci. Technol. 48 (2016) 51–62. doi:10.1016/J.TIFS.2015.12.001.

[20] J. Gómez-Estaca, C. López-de-Dicastillo, P. Hernández-Muñoz, R. Catalá, R. Gavara, Advances in antioxidant active food packaging, Trends Food Sci. Technol. 35 (2014) 42–51. doi:10.1016/J.TIFS.2013.10.008.

[21] A. Mousavi Khaneghah, S.M.B. Hashemi, S. Limbo, Antimicrobial agents and packaging systems in antimicrobial active food packaging: An overview of

approaches and interactions, Food Bioprod. Process. 111 (2018) 1–19. doi:10.1016/J.FBP.2018.05.001.

[22] G. Kavoosi, B. Nateghpoor, S.M.M. Dadfar, S.M.A. Dadfar, Antioxidant, antifungal, water binding, and mechanical properties of poly(vinyl alcohol) film incorporated with essential oil as a potential wound dressing material, J. Appl. Polym. Sci. 131 (2014) 1–8. doi:10.1002/app.40937.

[23] C. Chen, Z. Xu, Y. Ma, J. Liu, Q. Zhang, Z. Tang, K. Fu, F. Yang, J. Xie, Properties, vapour-phase antimicrobial and antioxidant activities of active poly(vinyl alcohol) packaging films incorporated with clove oil, Food Control. 88 (2018) 105–112. doi:10.1016/J.FOODCONT.2017.12.039.

[24] C. Chenwei, T. Zhipeng, M. Yarui, Q. Weiqiang, Y. Fuxin, M. Jun, X. Jing, Physicochemical, microstructural, antioxidant and antimicrobial properties of active packaging films based on poly(vinyl alcohol)/clay nanocomposite incorporated with tea polyphenols, Prog. Org. Coatings. 123 (2018) 176–184. doi:10.1016/J.PORGCOAT.2018.07.001.

[25] Q. Ma, Y. Ren, L. Wang, Investigation of antioxidant activity and release kinetics of curcumin from tara gum/ polyvinyl alcohol active film, Food Hydrocoll. 70 (2017) 286–292. doi:10.1016/j.foodhyd.2017.04.018.

[26] S. Do Yoon, Y.M. Kim, B. Il Kim, J.Y. Je, Preparation and antibacterial activities of chitosan-gallic acid/polyvinyl alcohol blend film by LED-UV irradiation, J. Photochem. Photobiol. B Biol. 176 (2017) 145–149. doi:10.1016/j.jphotobiol.2017.09.024.

[27] S.R. Kanatt, M.S. Rao, S.P. Chawla, A. Sharma, Active chitosan-polyvinyl alcohol films with natural extracts, Food Hydrocoll. 29 (2012) 290–297. doi:10.1016/j.foodhyd.2012.03.005.

[28] ASTM, Standard Test Method for Tensile Properties of Thin Plastic Sheeting, ASTM D882-02, Am. Soc. Test. Mater. 14 (2002) 1–10.

[29] C. Methods, Standard Test Methods for Water Vapor Transmission of Shipping Containers —, 95 (2003) 4–6. doi:10.1520/D4279-95R09.2.

[30] A. Cano, A. Jiménez, M. Cháfer, C. Gónzalez, A. Chiralt, Effect of amylose:amylopectin ratio and rice bran addition on starch films properties, Carbohydr. Polym. 111 (2014) 543–555. doi:10.1016/j.carbpol.2014.04.075.

[31] T.P. Film, Standard Test Method for Determination of Oxygen Gas Transmission Rate , Permeability and Permeance at Controlled Relative Humidity Through Barrier Materials Using a Coulometric Detector 1, Water. 98 (2004) 1–6. doi:10.1520/F1927-07.

[32] Á. Perdones, A. Chiralt, M. Vargas, Properties of film-forming dispersions and films based on chitosan containing basil or thyme essential oil, Food Hydrocoll. 57 (2016) 271–279. doi:10.1016/j.foodhyd.2016.02.006.

[33] X. Song, G. Zuo, F. Chen, Effect of essential oil and surfactant on the physical and antimicrobial properties of corn and wheat starch films, Int. J. Biol. Macromol. 107 (2018) 1302–1309. doi:10.1016/j.ijbiomac.2017.09.114.

[34] M. Wiśniewska, V. Bogatyrov, I. Ostolska, K. Szewczuk-Karpisz, K. Terpiłowski, A. Nosal-Wiercińska, Impact of poly(vinyl alcohol) adsorption on the surface characteristics of mixed oxide MnxOy–SiO2, Adsorption. 22 (2016) 417–423. doi:10.1007/s10450-015-9696-2.

[35] H. Abral, A. Hartono, F. Hafizulhaq, D. Handayani, E. Sugiarti, O. Pradipta, Characterization of PVA/cassava starch biocomposites fabricated with and without sonication using bacterial cellulose fiber loadings, Carbohydr. Polym. 206 (2019) 593–601. doi:10.1016/j.carbpol.2018.11.054.

[36] A. Altan, Z. Aytac, T. Uyar, Carvacrol loaded electrospun fibrous films from zein and poly(lactic acid) for active food packaging, Food Hydrocoll. 81 (2018) 48–59. doi:10.1016/j.foodhyd.2018.02.028.

[37] L. Buendía−Moreno, M.J. Sánchez−Martínez, V. Antolinos, M. Ros−Chumillas, L. Navarro−Segura, S. Soto−Jover, G.B. Martínez−Hernández, A. López−Gómez, Active cardboard box with a coating including essential oils entrapped within cyclodextrins and/or hallosyte nanotubes. A case study for fresh tomato storage, Food Control. 107 (2020) 106763. doi:10.1016/j.foodcont.2019.106763.

[38] L.M. Neira, J.F. Martucci, N. Stejskal, R.A. Ruseckaite, Time-dependent evolution of properties of fish gelatin edible films enriched with carvacrol during storage, Food Hydrocoll. 94 (2019) 304–310. doi:10.1016/j.foodhyd.2019.03.020.

[39] G.G.G. Trindade, G. Thrivikraman, P.P. Menezes, C.M. França, B.S. Lima, Y.M.B.G. Carvalho, E.P.B.S.S. Souza, M.C. Duarte, S. Shanmugam, L.J. Quintans-Júnior, D.P. Bezerra, L.E. Bertassoni, A.A.S. Araújo, Carvacrol/β-cyclodextrin inclusion complex inhibits cell proliferation and migration of prostate cancer cells, Food Chem. Toxicol. 125 (2019) 198–209. doi:10.1016/j.fct.2019.01.003.

[40] H.Y. Wang, S.S. Lu, Z.R. Lun, Glass transition behavior of the vitrification solutions containing propanediol, dimethyl sulfoxide and polyvinyl alcohol, Cryobiology. 58 (2009) 115–117. doi:10.1016/j.cryobiol.2008.10.131.

[41] B. Rimez, H. Rahier, G. Van Assche, T. Artoos, M. Biesemans, B. Van Mele, The thermal degradation of poly(vinyl acetate) and poly(ethylene-co-vinyl acetate), Part I: Experimental study of the degradation mechanism, Polym. Degrad. Stab. 93 (2008) 800–810. doi:10.1016/j.polymdegradstab.2008.01.010.

729 [42] B. Rimez, H. Rahier, G. Van Assche, T. Artoos, B. Van Mele, The thermal
730 degradation of poly(vinyl acetate) and poly(ethylene-co-vinyl acetate), Part II:
731 Modelling the degradation kinetics, Polym. Degrad. Stab. 93 (2008) 1222–1230.
732 doi:10.1016/j.polymdegradstab.2008.01.021.

733 [43] D. Cristancho, Y. Zhou, R. Cooper, D. Huitink, F. Aksoy, Z. Liu, H. Liang, J.M.
734 Seminario, Degradation of polyvinyl alcohol under mechanothermal stretching, J.
735 Mol. Model. 19 (2013) 3245–3253. doi:10.1007/s00894-013-1828-6.

736 [44] K.P. Safna Hussan, M.S. Thayyil, T.V. Jinitha, J. Kolte, Development of an
737 ionogel membrane PVA/[EMIM] [SCN] with enhanced thermal stability and ionic
738 conductivity for electrochemical application, J. Mol. Liq. 274 (2019) 402–413.
739 doi:10.1016/J.MOLLIQ.2018.10.128.

740 [45] I. Restrepo, C. Medina, V. Meruane, A. Akbari-Fakhrabadi, P. Flores, S.
741 Rodríguez-Llamazares, The effect of molecular weight and hydrolysis degree of
742 poly(vinyl alcohol)(PVA) on the thermal and mechanical properties of poly(lactic
743 acid)/PVA blends, Polimeros. 28 (2018) 169–177. doi:10.1590/0104-
744 1428.03117.

745 [46] P. Tongnuanchan, S. Benjakul, T. Prodpran, Properties and antioxidant activity
746 of fish skin gelatin film incorporated with citrus essential oils, Food Chem. 134
747 (2012) 1571–1579. doi:10.1016/j.foodchem.2012.03.094.

748 [47] L. Atarés, C. De Jesús, P. Talens, A. Chiralt, Characterization of SPI-based
749 edible films incorporated with cinnamon or.pdf, J. Food Eng. 99 (2010) 384–391.
750 doi:10.1016/j.jfoodeng.2010.03.004.

751 [48] S.M. Ojagh, M. Rezaei, S.H. Razavi, S.M.H. Hosseini, Effect of chitosan
752 coatings enriched with cinnamon oil on the quality of refrigerated rainbow trout,
753 Food Chem. 120 (2010) 193–198. doi:10.1016/j.foodchem.2009.10.006.

[49] C. Valencia-Sullca, M. Jiménez, A. Jiménez, L. Atarés, M. Vargas, A. Chiralt, Influence of liposome encapsulated essential oils on properties of chitosan films, Polym. Int. 65 (2016) 979–987. doi:10.1002/pi.5143.